

RESEARCH ARTICLE

SNR optimized ^{31}P functional MRS to detect mitochondrial and extracellular pH change during visual stimulation

Arjan D. Hendriks  | Wybe J.M. van der Kemp  | Peter R. Luijten | Natalia Petridou | Dennis W.J. Klomp

Department of Radiology, University Medical Center Utrecht, Utrecht, the Netherlands

Correspondence

Arjan Hendriks and Dennis Klomp, UMC Utrecht, Room Q.02.4.312, Heidelberglaan 100 (P.O. Box 85500), 3584 CX Utrecht, The Netherlands.

Email: a.d.hendriks-6@umcutrecht.nl; d.w.j.klomp-2@umcutrecht.nl

Funding information

Dutch Research Council (NWO), Grant/Award Number: 13339

Summary: Energy metabolism of the human visual cortex was investigated by performing ^{31}P functional MRS.

Introduction: The human brain is known to be the main glucose demanding organ of the human body and neuronal activity can increase this energy demand. In this study we investigate whether alterations in pH during activation of the brain can be observed with MRS, focusing on the mitochondrial inorganic phosphate (Pi) pool as potential marker of energy demand.

Methods: Six participants were scanned with 16 consecutive ^{31}P -MRSI scans, which were divided in 4 blocks of 8:36 minutes of either rest or visual stimulation. Since the signals from the mitochondrial compartments of Pi are low, multiple approaches to achieve high SNR ^{31}P measurements were combined. This included: a close fitting ^{31}P RF coil, a 7 T-field strength, Ernst angle acquisitions and a stimulus with a large visual angle allowing large spectroscopy volumes containing activated tissue.

Results: The targeted resonance downfield of the main Pi peak could be distinguished, indicating the high SNR of the ^{31}P spectra. The peak downfield of the main Pi peak is believed to be connected to mitochondrial performance. In addition, a BOLD effect in the PCr signal was observed as a signal increase of 2–3% during visual stimulation as compared to rest. When averaging data over multiple volunteers, a small subtle shift of about 0.1 ppm of the downfield Pi peak towards the main Pi peak could be observed in the first 4 minutes of visual stimulation, but no longer in the 4 to 8 minute scan window. Indications of a subtle shift during visual stimulation were found, but this effect remains small and should be further validated.

Conclusion: Overall, the downfield peak of Pi could be observed, revealing opportunities and considerations to measure specific acidity (pH) effects in the human visual cortex.

KEYWORDS

mitochondrial Pi, ^{31}P MRS, fMRS, pH, phosphorus spectroscopy, visual cortex

Abbreviations: BOLD, Blood-oxygenation-level dependent; DPG, 2,3-diphosphoglycerate; MRSI, Magnetic resonance spectroscopic imaging; PC, Phosphocholine; PCr, Phosphocreatine; Pi, Inorganic phosphate; P_i , Intracellular inorganic phosphate; $\text{P}_{\text{mi/ex}}$, Mitochondrial and/or extracellular inorganic phosphate; RF, Radio frequency; SNR, Signal-to-noise ratio.

This is an open access article under the terms of the Creative Commons Attribution-NonCommercial License, which permits use, distribution and reproduction in any medium, provided the original work is properly cited and is not used for commercial purposes.

© 2019 The Authors. *NMR in Biomedicine* Published by John Wiley & Sons Ltd

1 | INTRODUCTION

The human brain consumes a considerable amount of energy, and is known to be the main glucose demanding organ of the human body.¹ Neuronal activity can increase this energy demand, and can cause local pH changes via several mechanisms.^{2,3} So, studying energy metabolism in the human brain could potentially provide a direct assessment of neuronal integrity and functioning.

³¹P magnetic resonance spectroscopy (³¹P MRS) is often used to study energy metabolism in-vivo and non-invasively,^{4,5} for it can detect the energy metabolism products such as adenosine triphosphate (ATP), phosphocreatine (PCr), and inorganic phosphate (Pi). Moreover, using saturation transfer techniques, exchange rates between ATP and Pi can be determined,⁶ and acidity can be derived using the pH sensitive resonance position of the Pi signal. During muscle exercise, substantial alterations in PCr and Pi levels can be observed, as well as a clear shift of the frequency of the Pi signal that coincides with pH alteration. Even distinctions between Pi pools in mitochondrial, intracellular and extracellular compartments are visible due to their characteristic pH and thereby peak position in the ³¹P MR spectrum.⁷

Over the past decades, studies have observed small alterations in ³¹P MRS signal levels or pH changes in the brain during activation.⁸⁻¹⁶ However, these small changes are in marked contrast to the large activation-induced alterations of ³¹P MR signals in muscle. Under baseline hypoxia, neither the PCr/ATP and Pi/(Pi+ PCr) ratios nor intracellular pH levels in the brain were affected,¹⁷ despite the fact that blood oxygen saturation ranged from 0.95 to 0.83 reducing the blood's capacity to deliver O₂ to the brain as required for energy metabolism. Only chemical exchange rates during visual stimulation have been observed⁶ and recently confirmed.¹⁸ In general, it is widely recognized that the energy metabolism of the brain is strongly regulated and intracellular pH levels are controlled, for example through buffer processes such as the CO₂/HCO₃⁻ system. Because of these regulatory mechanisms, the magnitude of the neuronal activity induced pH changes is very small, therefore with MRS it could possibly only be detected as a small shift in peak frequency or minimal change in peak amplitude of Pi. A subtle shift in the intracellular Pi peak or amplitude alteration is challenging to observe, as the ³¹P MRS peaks will get narrower line widths and higher amplitudes during stimulation caused by BOLD effects. Moreover, signals of 2,3-DPG (2,3-diphosphoglycerate) from blood may contaminate the spectrum as demonstrated in cardiac MRS, as these have resonances close to the Pi peak.^{19,20}

In our study, we propose an alternative means to observe alterations in pH during activation of the brain. Rather than focusing on the total observed Pi pool, which is predominantly intra cellular, our study aims to observe pH alterations in the mitochondria. Distinction between mitochondrial Pi and intracellular Pi is possible due to their different acidic environments: pH of 7.8 in mitochondria (as derived from cell work)²¹ versus 7.05 of the intracellular pool.²² When the chemical shift of PCr is normalized at 0 ppm, Pi at a pH of 7.8 corresponds to a chemical shift of 5.5 ppm, and Pi at a pH of 7.05 corresponds to 4.9 ppm. The spectral resolution is more than sufficient at a field strength of 7 T to distinguish these two signals that have a chemical shift difference of 0.6 ppm (i.e. similar difference as phosphocholine at 6.2 ppm and phosphoethanolamine at 6.8 ppm that have demonstrated clear distinction at 7 T).²³

However, the pool size of Pi in both mitochondria and extracellular space is substantially less than intracellular Pi. Therefore, the signal to noise ratio (SNR) has to be increased. With the use of SNR optimized RF coils for calf muscle ³¹P MRS at 7 T, it has been demonstrated that the mitochondrial Pi pool reflects about 13% of the total observed intracellular Pi pool.⁷ In fact, when taking a closer look at the first ³¹P spectra obtained from the human brain at 7 T,²⁴ a small peak downfield from the main Pi peak can be observed. This could very well be mitochondrial Pi, albeit it was not labeled by the authors as such. Besides mitochondrial Pi, alkaline Pi signal has previously also been assigned to be extracellular Pi in ³¹P MR spectra obtained in the human brain.^{25,26} The exact contribution of the mitochondrial and extracellular compartments to the alkaline Pi signal in the brain is not well established. Overall, when optimizing SNR of ³¹P MRS in the human brain, the mitochondrial and/or extracellular Pi pool may be detected.

The SNR of the downfield Pi signal can be improved at 7 T in several steps. First, the volume of activated tissue can be enlarged. A large volume of activated tissue would enable the use of a large spectroscopy voxel size, resulting in an additional increase in SNR similar as recently observed for enlarged voxel measurements of γ -aminobutyric acid (GABA) using a setup with a large visual angle.²⁷ Secondly, the RF coil can be optimized for higher SNR. Using a tight-fit volume resonator, a uniform excitation can be obtained while assuring highest SNR in the center of the brain.²⁸ Moreover, when compared to surface coil transceivers, the uniform reception will reduce potential contamination from ³¹P signals from the large vessels close to the skull. Finally, it was demonstrated that the T₁ relaxation time of mitochondrial Pi is about four-fold shorter than intracellular Pi,⁷ therefore short TR sequences can be used that maximize the SNR per unit of time.

In this study, the above mentioned SNR optimization steps were implemented to investigate the behavior of the downfield Pi peak in the human brain of six healthy volunteers during visual stimulation.

2 | METHODS

Six participants (5 male, 1 female, 24–43 years old) were scanned in a 7 Tesla Achieva system (Philips, Best, the Netherlands). The first participant was scanned three times: twice to test the setup and scan protocols, and a third time to acquire data with an identical scan protocol as for the rest of the participants. All participants provided written informed consent, and the study was approved by the medical ethics committee of the University Medical Center Utrecht.

A dedicated custom coil setup was used with a large screen for projection of a stimulus with a large visual angle (Figure 1). The visual angle was around 40 degrees in height and more than 70 degrees in width. The transmit/receive coil was a tight fit (inner diameter = 23 cm), shielded quadrature birdcage coil, double tuned to both the ^1H and ^{31}P frequency. Ceramic floating cable traps tuned for ^{31}P and ^1H were used in series for both cables that run from the ^1H and ^{31}P coil, via an RF splitter, to the narrow band transmit receive switches, quadrature hybrids and preamplifiers of the MRI system.

An initial anatomical ^1H gradient echo scan was made at the start of the session. This scan contained 3 orthogonal slices and was used for planning. The parameters of this scan were: TE = 2.0 ms, TR = 42 ms, 45 degrees flip angle, 3 orthogonal slices (stacks), FOV = 500x500x3 mm³, spatial resolution = 2x2x3 mm³, and a total scan time of 10.7 s.

B_0 shimming of the visual cortex was performed by acquiring a 3D B_0 map, and subsequently updating the currents in the shim coils with the calculated values from the first and second order harmonics that fit to the B_0 maps. The B_0 maps were obtained with TE = 1.54 ms, delta TE = 1 ms, TR = 4 ms, FOV = 240x180x157 mm³, spatial resolution = 3.75x3.75x3.75 mm³, and a total scan time of 16.2 s. After the B_0 shim update, the water frequency was determined from the visual cortex using the standard semi-LASER sequence implemented by the vendor.²⁹ The frequency was used to fix the carrier frequency of the ^{31}P MR system during the remainder of the scan session.

A pulse-acquire ^{31}P MR sequence was used and configured with a short TR of 100 ms to obtain highest SNR per unit of time, while providing an acquisition window of 80 ms (512 datapoints at 6400 Hz) and a spectral resolution of 0.1 ppm. An Ernst-angle of 20 degrees was used, based on the estimated shortened T_1 value of mitochondrial Pi of 1.4 s in muscle, as obtained from literature.⁷ The excitation pulse duration was set to 109 μs , and the pulse was amplified using the 4 kW RF amplifier of the MR system. Gradient phase encoding steps of 400 μs were included to the sequence to provide 3D MR Spectroscopic Imaging (MRSI) in order to spatially distinguish the ^{31}P MR spectrum of the stimulated visual cortex from the remainder of the brain (280x280x280 mm³ FOV, matrix size 8x8x8, 35x35x35 mm³ nominal voxelsize). Hanning weighted averaging³⁰ was applied with 6 averages of the center of k-space resulting in a scan time of 2:09 minutes. The weighted acquisition scheme lead to an actual voxelsize (as defined by the 64% level of the spatial response function) of 62 mm isotropic. For each participant a total of 16 consecutive ^{31}P MRSI scans were acquired.

Visual stimuli were projected in blocks of 4 scans (4 rest, 4 stimulus, 4 rest, 4 stimulus), as is shown in Figure 2. The visual stimulus consisted of a curved-line pattern reversing contrast at 8 Hz. The curved lines were oriented in different directions, to target and stimulate a big pool of neurons with varying orientation preference.³¹ The stimulus was presented for 8:36 min (4 scans) and was repeated after the rest period. The first subject was scanned three times to test the scan protocols. In the first two sessions of the first subject a standard 8 Hz contrast reversing checkerboard pattern was used as visual stimulus. In the final session an identical visual stimulus was used as for the rest of the participants. Both visual stimulus types were presented with a large visual angle, as was possible by using the custom coil setup.

After scanning, in post processing steps, the k-space data was weighted in accordance with the Hanning weighted sampling strategy used during acquisition. After Fourier transform, 1 voxel located in the visual cortex was selected from each 3D MRSI scan. The voxel was selected based on the location of the primary visual cortex on an anatomical background scan of the brain. The voxel selection and MRSI grid is displayed in Figure 3. The resulting spectra from the selected voxel were phased using a fixed first order phase setting corresponding to the delay of 503 μs between the center of excitation and the center of the first acquired data point. Manual zero order phasing was performed and fixed

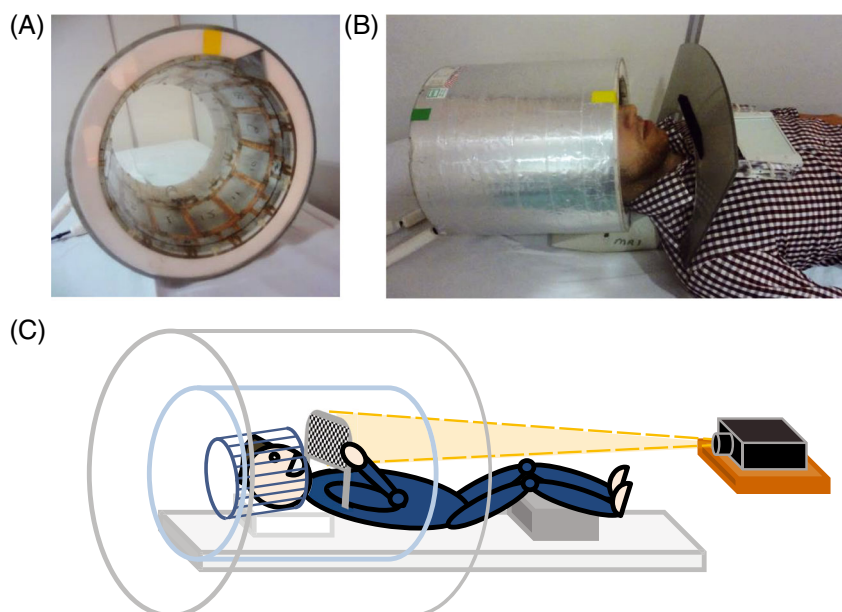


FIGURE 1 The coil setup, which is equipped with a screen for visual stimulation. Displayed are a photograph of the ^1H - ^{31}P transmit-receive coil (A), a photograph of the coil when the screen is mounted (B) and a schematic overview of setup during signal acquisition (C). Note that no mirrors or prism glasses are required for this setup, which enhances the visual angle of view with respect to the projected stimulus

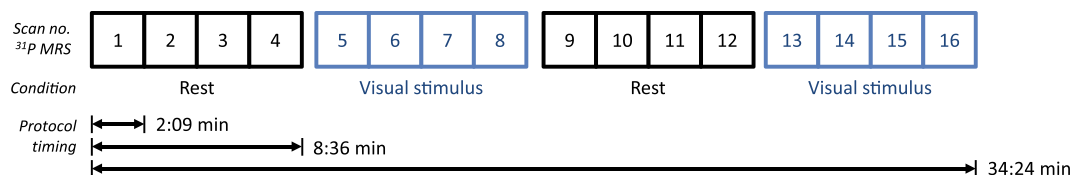


FIGURE 2 Overview of the ^{31}P MRS scan protocol. Sixteen ^{31}P MRS scans of 2:09 minutes are acquired in 6 participants. Visual stimuli were projected in blocks of 4 scans (4 rest, 4 stimulus, 4 rest, 4 stimulus). In total, the ^{31}P MRS scans had a duration of 34:24 minutes

to the same setting for all spectra obtained from the same participant. Next, datasets were zero-filled to 4096 data points and apodized with a 10 Hz Lorentzian. The spectra were aligned to the large PCr peak for each participant individually. Afterwards the PCr peak was also aligned among datasets of different participants. An indication of the SNR of the PCr peak is given, by dividing the maximum amplitude of the PCr peak by the standard deviation of a noise region in the spectrum. Since the extract contribution of the mitochondrial and extracellular compartments to the alkaline Pi signal is not well established, the alkaline Pi signal in the figures was labeled as mitochondrial and/or extracellular Pi signal ($\text{Pi}_{\text{mi/ex}}$).

For the analysis, the spectra were averaged in three ways: First, four sets of 4 spectra were averaged for each individual participant (i.e. 4 rest, 4 stimulus, 4 rest and 4 stimulus). From these averaged spectra, the BOLD effect to PCr is assessed by plotting the PCr peak over time. Second, the 16 individual consecutive scans were averaged over the 6 participants to assess temporal behavior of the mitochondrial Pi pool and pH. Matching blocks of either rest or stimulation were averaged to visualize the first 2 minutes, second 2 minutes and end of the stimulation block, to investigate possible dynamic changes of metabolites during the experiment. Third, the spectra that were acquired in the same block (rest, stimulation, rest, stimulation) were averaged over all participants. The relative amplitude and peak position of the mitochondrial Pi peak as compared to the main intracellular Pi peak was assessed using Gaussian line fitting (jMRUI version 4.0) with fixed constraints and prior knowledge on peak position and line width.

3 | RESULTS

All included participants fitted in the RF coil and reported full visual view of the screen. In one participant the large visual field of view for visual stimulation is shown (Figure 1). The duration of the preparation steps such as planning and B_0 -shimming took less than 10 minutes, starting from the moment the participant was inside the MRI until the start of the first dynamic ^{31}P MRSI scan. In one of the 6 participants, the automatic frequency determination was off during the preparation steps, thereby causing an off resonance of 1 kHz as compared to the spectra acquired from the other participants. As this offset is well within the bandwidth of the 109 μs RF excitation pulse (9.2 kHz), the dataset was still included in all analyses.

In the first scan session of the first participant, the scan protocol was tested. Due to the high SNR of the ^{31}P spectra a clear resonance downfield of the main Pi peak was visible (Figure 4A). The fits of the two Pi peaks indicated that the signal integral of the downfield peak was 0.2 times the signal integral of the main Pi peak. The integral of the intracellular Pi peak was not found to be changing during the stimulation blocks. Upon

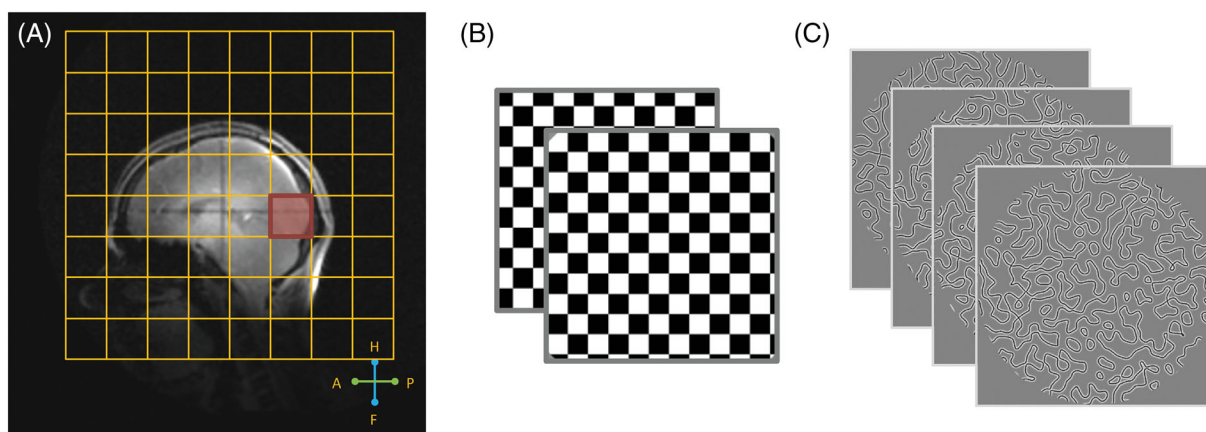


FIGURE 3 Voxel selection. The ^{31}P MRSI voxelgrid is displayed on an ^1H anatomical background (A). The nominal voxel size of the ^{31}P 3D MRSI scan is shown. The selected voxel in the primary visual cortex is marked in red. Two types of visual stimulus are used to stimulate the visual cortex: a traditional contrast reversing checkboard (B) and curved lines oriented in different directions (C)

closer inspection, the frequency of the intracellular Pi peak at 4.85 ppm corresponding to a pH of 7.01 did not shift, while the mitochondrial Pi peak shifted at max 0.1 ppm up field during visual stimulation, corresponding to a shift in pH from 7.55 to 7.41. In addition, a clear BOLD effect in the PCr signal was observed, reflected as a signal increase of approximately 15% when comparing the spectra obtained during rest with the ones obtained during visual stimulation with the contrast-reversing checkerboard (Figure 4C). Voxels outside of the visual cortex did not show a large influence of the BOLD effect on the PCr peak (Figure 5).

As the temporal resolution of the MRSI scans was 2 minutes, while rest and stimulation periods were 8 minutes, dynamic alterations of ^{31}P metabolites within the stimulation period can be investigated. In order to maximize SNR, data was averaged not only from all participants, but also from both rest and both stimulation events. Again, a subtle shift of about 0.1 ppm of the downfield Pi peak towards the main Pi peak could be observed in the first 2 minutes as well as in the second 2 minutes scan, but no longer in the 4 to 8 minute scan window (Figure 6).

In the ^{31}P spectra of the individual participants, the downfield Pi peak was visible in 5 out of 6 participants (Figure 7). The SNR of these spectra was not sufficient to detect a 0.1 ppm shift of the Pi peak over time. An indication of the SNR of the PCr peak (SNR_{PCr}) is noted in Figure 7 for each participant separately. On average the SNR_{PCr} was 64 ± 9 (mean \pm std). Note that this indication of SNR is not independent of linewidth, since it was calculated by dividing the maximum of the PCr peak by the standard deviation of a noise region. In one participant the carrier frequency was off, thereby missing the β -ATP peak, yet the SNR of the remaining peaks remained similar when compared to the SNR of the ^{31}P MR spectra from the other participants.

In the ^{31}P MRS datasets of the individual participants, the BOLD effect on the PCr peak was not clearly observed, however, when averaging over all participants, the signal intensity increased 2–3% during stimulation as compared to rest (Figure 8, inset). The alignment of the spectra between participants facilitated averaging spectra over participants, while maintaining the detection of the downfield peak of Pi (Figure 8). When comparing the averaged spectra of Figure 8 with Figure 4, clearly the SNR improved. Likewise, line broadening or a subtle shift of the downfield Pi peak over time of less than 0.1 ppm could be observed.

4 | DISCUSSION AND CONCLUSION

The energy metabolism of the visual cortex was investigated with ^{31}P MRS during visual stimulation with a large visual angle. Consequently, the spatial resolution could be reduced, or the voxel size increased to the enlarged stimulated area, in return for higher SNR and temporal resolution of the dynamic ^{31}P MRSI exams. Combined with Ernst-angle acquisitions, and a close fitting RF coil, a clear resonance downfield from the intracellular Pi peak can be observed within a temporal resolution of 2 minutes. Moreover, during visual stimulation, a subtle shift of at most 0.1 ppm of this peak can be observed, corresponding to a pH shift of -0.13 units when assigning the peak as Pi from either the mitochondria or the extra-cellular space.

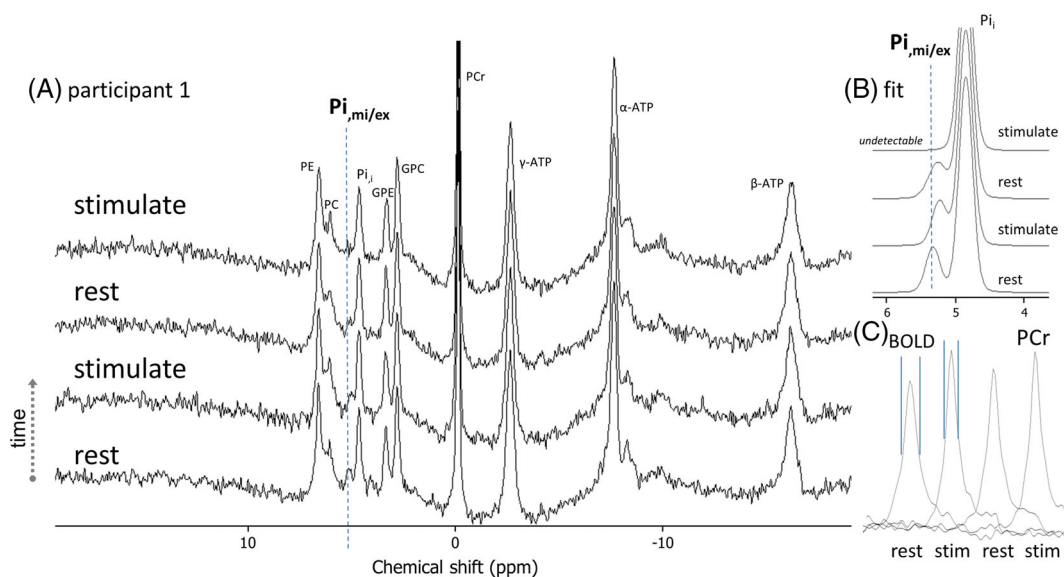


FIGURE 4 ^{31}P MR spectra from the first scan session of the first participant (A). These spectra are obtained during rest and during visual stimulation with a checkerboard reversing contrast at 8 Hz. Each spectrum is an average of 4 consecutive scans of 2 minutes. A clear peak downfield from the intracellular Pi peak is indicated by the striped line. Upon closer inspection of the $\text{Pi}_{\text{mi/ex}}$ peak, a small shift in frequency can be observed, particularly when comparing the first rest spectrum (bottom) with the first stimulus spectrum (second from the bottom). A zoom of the Pi-region is displayed (B), showing the fitted peaks. In addition, when comparing the rest spectra with the stimulus spectra, a line narrowing of the PCr peak can be observed (C), reflected as $\approx 15\%$ increase in PCr amplitude during stimulus

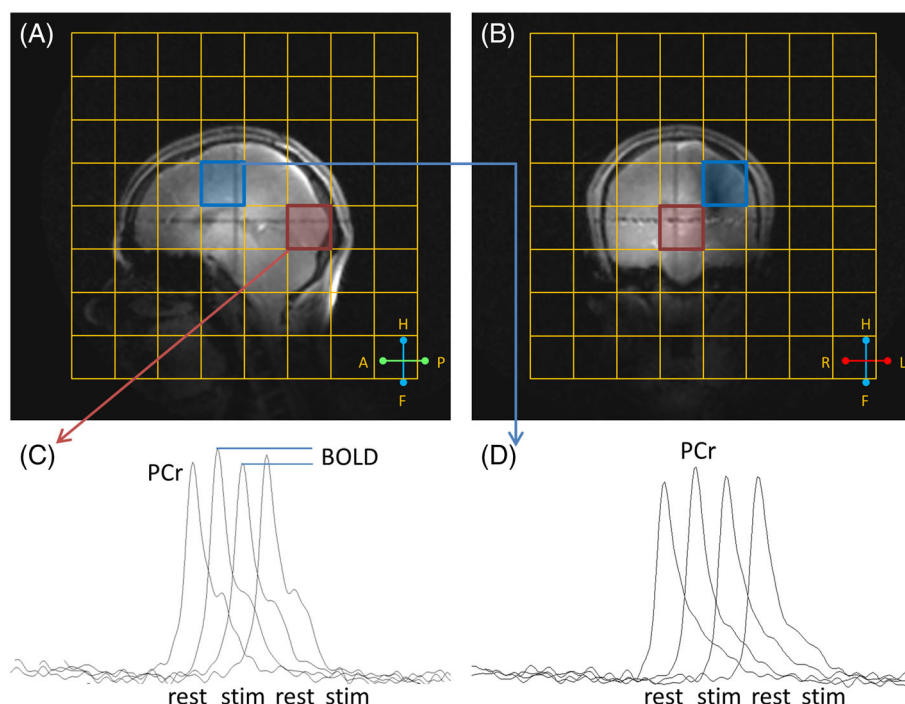


FIGURE 5 Comparison between MRSI voxels. The ^{31}P MRSI acquisition grid and the ^1H anatomical background are displayed (A,B). The selected voxel in the visual cortex is marked in red. The corresponding PCr peaks of this voxel are shown over time (C). Note that a BOLD effect is observable in the visual cortex. For comparison, the PCr peaks for a voxel outside of the visual cortex, marked in blue, are also shown (D). In that voxel, the presence or potential influence of a BOLD effect is less noticeable

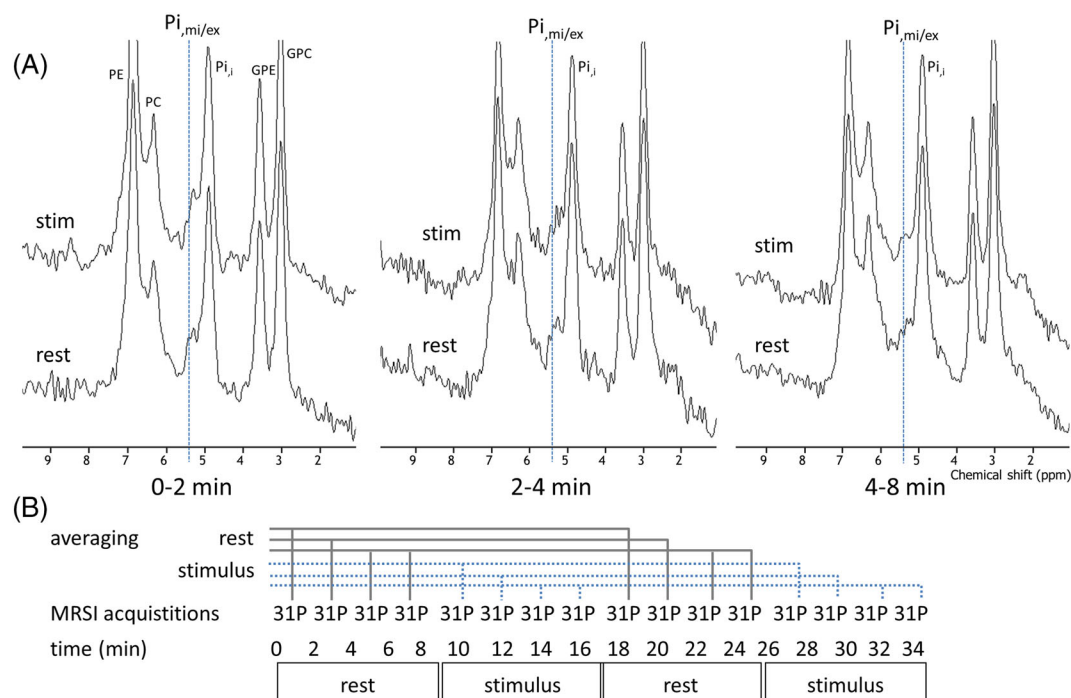


FIGURE 6 Dynamic ^{31}P MR spectra of the visual cortex, which are temporally matched and averaged over all six participants (A). The temporal averaging is shown schematically (B). The spectra are obtained during rest and visual stimulation, at a temporal resolution of 2 minutes. In the spectra obtained in the first two minutes, as well as the spectra obtained in the second 2 minutes, a shift or line splitting of the $\text{Pi}_{\text{mi/ex}}$ peak can be observed during visual stimulation when compared to the corresponding rest spectra. The shift is not observed in the averaged spectra of the final 4 minutes of activation when compared to rest

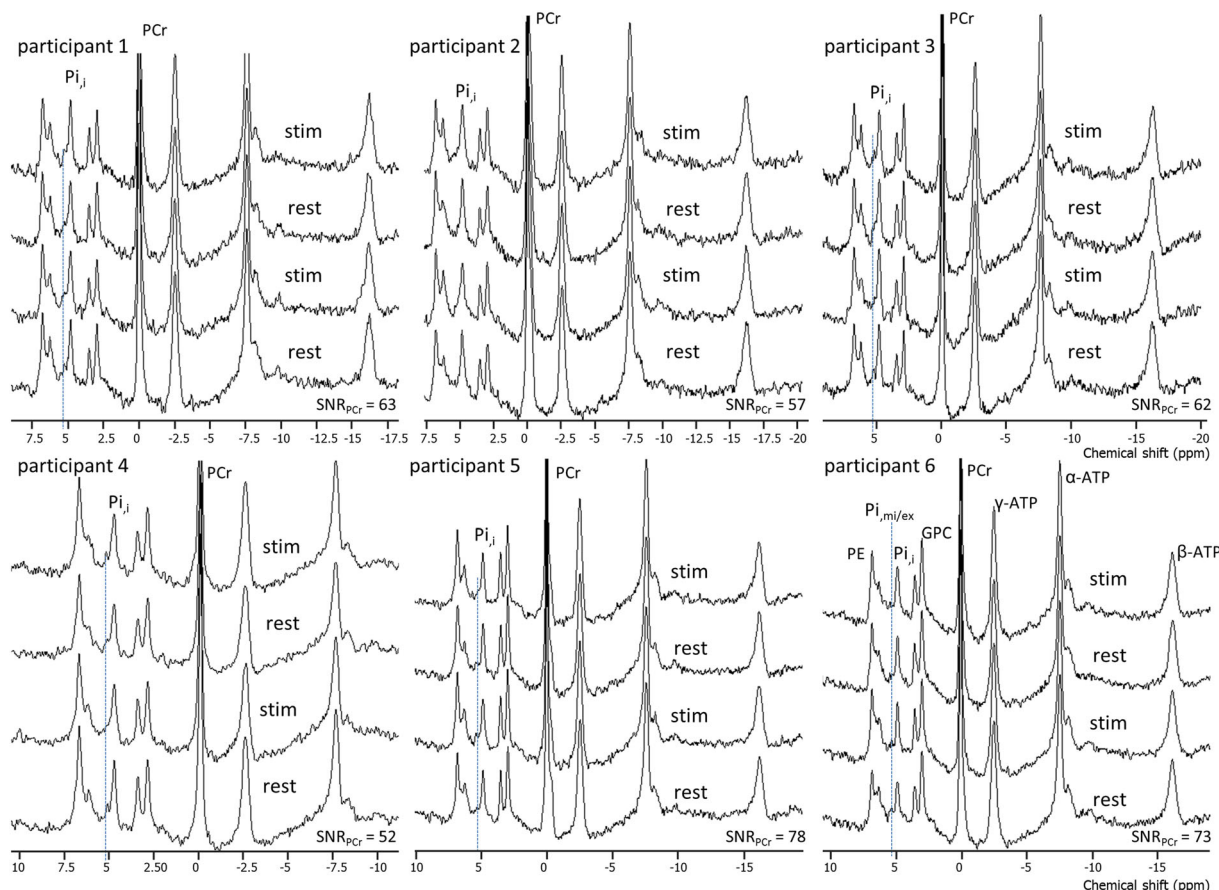


FIGURE 7 ^{31}P MR spectra of all participants individually. The spectra of the visual cortex of the brain are acquired dynamically during rest (lower), stimulus (second), rest (third) and stimulus (upper). The $\text{Pi}_{\text{mi/ex}}$ peak downfield from the Pi_{i} peak is clearly visible in participant 1, 3, 4, 5, and 6, highlighted by the striped line. Note that for participant 4 the spectra are not fully displayed (no $\beta\text{-ATP}$ peak), due to a 1 kHz offset during acquisition

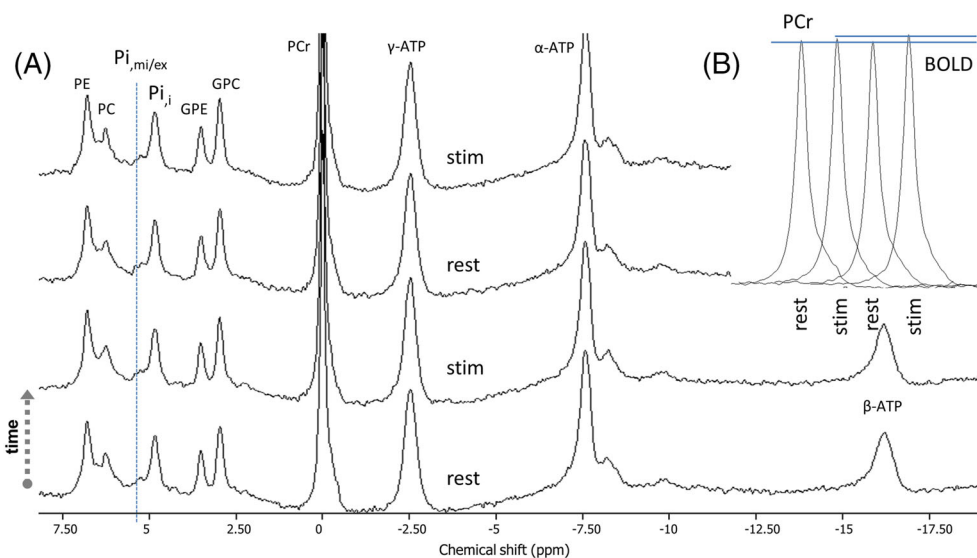


FIGURE 8 The average ^{31}P MR spectra across participants. Individual spectra were averaged over all six participants in blocks of 8 minutes of rest (rest) and visual stimulus (stim), resulting in an average spectrum for each block. The high SNR shows the mitochondrial/extracellular $\text{Pi}_{\text{mi/ex}}$ peak downfield from the intracellular Pi_{i} peak as indicated by the striped line (A). Line broadening, a small shift in frequency or even peak splitting of the $\text{Pi}_{\text{mi/ex}}$ peak can be observed when comparing the spectra over time. However, this effect is less prominent as compared to the effect in the spectra of individual participants (Figure 4) or the temporally averaged spectra (Figure 6). In addition, when comparing the rest spectra with the stimulus spectra, a BOLD effect reflected as a 2–3% increase in PCr during visual stimulation can be observed (B)

In this study we incorporated a relatively large voxel volume to obtain the SNR required to detect the downfield Pi peak. In addition, averaging over participants was another means to increase SNR, by using peak alignment of the large signal of PCr. This enabled studying subtle effects in peak position and line width at relatively high temporal resolution. Temporal resolution may be important, considering the possible saturation or habituation effects with the prolonged stimulation employed here. In fact, the shift in the downfield peak of Pi seems better visible in the first two minutes of activation than in the final 4 minutes of activation. In line with this finding, when averaging over the full block of 8 minutes for all participants, the difference between the rest and stimulus condition is less prominent. Still for the spectra of some individual participants and for the average over all participants a small shift in frequency, line broadening or even peak splitting of the $\text{Pi}_{\text{mi/ex}}$ is observed. These effects remain subtle and should therefore be further validated.

While it has been shown that receiver arrays could enhance SNR,³² large volumes deeper in the brain may benefit more from the use of a volume transceiver due to inherent RF phase distortions within the voxel. When using receiver arrays, the signal will be weighted non-uniformly throughout the voxel, which may bias towards larger signals of ^{31}P from blood originating close to those receiver arrays. Still, in specific areas and when aiming for smaller voxels, a receiver array can improve SNR. Some gain in SNR may also be found when obtaining a proper assessment of the T_1 of the downfield Pi spins in the brain to further optimize the Ernst angle. The signal of ^{31}P metabolites can also be enhanced by the use of the nuclear Overhauser effect (NOE).³³ More improvements in SNR can be achieved when going to higher magnetic fields, such as 9.4 T or in the near future to even higher field strengths.

Studies that use other approaches to measure pH changes in the brain, such as amide proton chemical exchange saturation transfer (APT-CEST), show that it is challenging to measure pH and that the expected pH differences could be smaller than 0.03 pH units.³⁴ However, the APT-CEST contrast is believed to predominantly originate from intracellular amides. In the current study it was aimed to specifically measure the pH in mitochondrial or extracellular compartments, so pH changes due to activation could be different there.

Two recent studies have been published that include high SNR ^{31}P MRSI protocols at 7 T. The first study does not observe any change in high-energy phosphates due to a visual stimulation,³⁵ but on the other hand does not include the downfield Pi peak in their analysis. The second study specifically targets the downfield Pi peak and shows the influences of the blood and CSF pool on this peak.³⁶

Although we have assigned the downfield Pi peak as mitochondrial Pi, it is expected to be composed of several other compounds as well. For instance, 2,3-DPG is highly abundant in blood and expresses itself at 7 T as two peaks in close proximity to the resonance of Pi and phosphocholine (PC). The absence of this peak in calf muscle was relatively simple to address, as PC levels are much lower in muscle therefore easier to identify the double 2,3-DPG peaks if they were above the noise floor. We have used phase encoding gradients and Hanning filtering to localize the voxel from the visual cortex, which due to point spread function and partial volume effects may still incorporate some signals from blood in the vasculature. Further reduction of the chance to include signals from the highly abundant vasculature close to the skull may be realized when using outer volume suppression by means of a crusher coil.³⁷ Another possibility could be that the signal comes from extracellular Pi at a much higher pH level than the intracellular Pi, or similar pH level as the mitochondrial Pi. Diffusion weighted spectroscopy may be applied to reduce the content from extracellular Pi. It should be noted that these diffusion techniques require stronger gradients considering the lower gyromagnetic ratio of ^{31}P over ^1H , and that SNR will go down.

We have shown that even with very high SNR and strong visual stimulation, energy metabolite levels remain highly intact. Yet, over 2 minutes of activation a subtle pH shift from 7.55 to 7.41 can be observed when assigning the downfield peak of Pi as mitochondrial or extracellular Pi. This drop in pH matches observations of lactate increase, as reported with ^1H MRS before.^{3,38} However, considering the substantial BOLD effect reflecting local alterations in oxygenation and high levels of glucose consumption of the brain, stronger effects in ^{31}P signals would be expected in close proximity to the neurons. The large voxel in our study will lead to partial volume effects of grey and white matter, which in total may have the buffering capacity to maintain the energy metabolite levels and environment constant. Longer and stronger activation strategies can be applied to study this buffer capacity. Or, when higher fields become available, reduced voxel sizes may be used to increase neuron density, which in that case can be helped by receiver arrays to provide the required SNR. Overall, the found small shift in frequency of the downfield peak of Pi is at the edge of what we can measure with the current setup, in terms of SNR and spectral resolution. The influence of phase corrections on the peak position was minimized, by fixing both zero and first order phase corrections. Still, the changes remain subtle, and further validation of the results is required.

In conclusion, energy metabolism of the human visual cortex was investigated by performing ^{31}P functional MRS. We focused on the mitochondrial inorganic phosphate pool as a potential marker of energy demand. The targeted resonance downfield of the main Pi peak could be distinguished, due to the high SNR of the ^{31}P spectra. Additionally, a BOLD effect in the PCr signal was observed. A small subtle shift of about 0.1 ppm of the downfield Pi peak towards the main Pi peak could be observed, especially in the first 4 minutes. When averaging over larger time periods the results were less prominent, indicating a time dependency. The effects are subtle and should be further validated. Overall, this study revealed potential opportunities to measure activation evoked changes in specific acidity (pH), but also emphasizes the need for higher SNR measurements to be able to study these processes in more detail.

ACKNOWLEDGEMENT

This work was supported in part by the Dutch Research Council (NWO), Vidi Grant 13339 (Petridou).

ORCID

Arjan D. Hendriks  <https://orcid.org/0000-0002-0363-2471>

Wybe J.M. van der Kemp  <https://orcid.org/0000-0003-1123-2352>

REFERENCES

1. Mergenthaler P, Lindauer U, Dienel GA, Meisel A. Sugar for the brain: the role of glucose in physiological and pathological brain function. *Trends Neurosci.* 2013;36(10):587-597.
2. Chesler M. Regulation and modulation of pH in the brain. *Physiol Rev.* 2003;83(4):1183-1221.
3. Magnotta VA, Heo HY, Dlouhy BJ, et al. Detecting activity-evoked pH changes in human brain. *Proc Natl Acad Sci U S A.* 2012;109(21):8270-8273.
4. Prompers JJ, Jeneson JA, Drost MR, Oomens CC, Strijkers GJ, Nicolay K. Dynamic MRS and MRI of skeletal muscle function and biomechanics. *NMR Biomed.* 2006;19(7):927-953.
5. Valkovic L, Chmelik M, Krssak M. In-vivo(31)P-MRS of skeletal muscle and liver: a way for non-invasive assessment of their metabolism. *Anal Biochem.* 2017;529:193-215.
6. Chen W, Zhu XH, Adriany G, Ugurbil K. Increase of creatine kinase activity in the visual cortex of human brain during visual stimulation: a 31P magnetization transfer study. *Magn Reson Med.* 1997;38(4):551-557.
7. Kan HE, Klomp DW, Wong CS, et al. In vivo 31P MRS detection of an alkaline inorganic phosphate pool with short T1 in human resting skeletal muscle. *NMR Biomed.* 2010;23(8):995-1000.
8. Barreto FR, Costa TB, Landim RC, Castellano G, Salmon CE. 31P-MRS using visual stimulation protocols with different durations in healthy young adult subjects. *Neurochem Res.* 2014;39(12):2343-2350.
9. Kato T, Murashita J, Shioiri T, Hamakawa H, Inubushi T. Effect of photic stimulation on energy metabolism in the human brain measured by 31P-MR spectroscopy. *J Neuropsychiatry Clin Neurosci.* 1996;8(4):417-422.
10. Mochel F, N'Guyen TM, Deelchand D, et al. Abnormal response to cortical activation in early stages of Huntington disease. *Movement Disorders: Official Journal of the Movement Disorder Society.* 2012;27(7):907-910.
11. Murashita J, Kato T, Shioiri T, Inubushi T, Kato N. Age-dependent alteration of metabolic response to photic stimulation in the human brain measured by 31P MR-spectroscopy. *Brain Res.* 1999;818(1):72-76.
12. Murashita J, Kato T, Shioiri T, Inubushi T, Kato N. Altered brain energy metabolism in lithium-resistant bipolar disorder detected by photic stimulated 31P-MR spectroscopy. *Psychol Med.* 2000;30(1):107-115.
13. Rango M, Bonifati C, Bresolin N. Parkinson's disease and brain mitochondrial dysfunction: a functional phosphorus magnetic resonance spectroscopy study. *J Cereb Blood Flow Metab.* 2006;26(2):283-290.
14. Rango M, Bozzali M, Prella A, Scarlato G, Bresolin N. Brain activation in normal subjects and in patients affected by mitochondrial disease without clinical central nervous system involvement: a phosphorus magnetic resonance spectroscopy study. *J Cereb Blood Flow Metab.* 2001;21(1):85-91.
15. Rango M, Castelli A, Scarlato G. Energetics of 3.5 s neural activation in humans: a 31P MR spectroscopy study. *Magn Reson Med.* 1997;38(6):878-883.
16. Sappey-Marini D, Calabrese G, Fein G, Hugg JW, Biggins C, Weiner MW. Effect of photic stimulation on human visual cortex lactate and phosphates using 1H and 31P magnetic resonance spectroscopy. *J Cereb Blood Flow Metab.* 1992;12(4):584-592.
17. Vidyasagar R, Kauppinen RA. 31P magnetic resonance spectroscopy study of the human visual cortex during stimulation in mild hypoxic hypoxia. *Exp Brain Res.* 2008;187(2):229-235.
18. Chen C, Stephenson MC, Peters A, Morris PG, Francis ST, Gowland PA. 31 P magnetization transfer magnetic resonance spectroscopy: assessing the activation induced change in cerebral ATP metabolic rates at 3 T. *Magn Reson Med.* 2018;79(1):22-30.
19. Rodgers CT, Clarke WT, Snyder C, Vaughan JT, Neubauer S, Robson MD. Human cardiac 31P magnetic resonance spectroscopy at 7 tesla. *Magn Reson Med.* 2014;72(2):304-315.
20. van der Kemp WJM, Klomp DWJ, Wijnen JP. 31 P T2 s of phosphomonoesters, phosphodiesteres, and inorganic phosphate in the human brain at 7T. *Magn Reson Med.* 2018;80(1):29-35.
21. Porcelli AM, Ghelli A, Zanna C, Pinton P, Rizzuto R, Rugolo M. pH difference across the outer mitochondrial membrane measured with a green fluorescent protein mutant. *Biochem Biophys Res Commun.* 2005;326(4):799-804.
22. Vorstrup S, Jensen KE, Thomsen C, Henriksen O, Lassen NA, Paulson OB. Neuronal pH regulation: constant normal intracellular pH is maintained in brain during low extracellular pH induced by acetazolamide--31P NMR study. *J Cereb Blood Flow Metab.* 1989;9(3):417-421.
23. van der Kemp WJ, Stehouwer BL, Runge JH, et al. Glycerophosphocholine and Glycerophosphoethanolamine are not the Main sources of the in vivo31P MRS phosphodiester signals from healthy Fibroglandular breast tissue at 7 T. *Front Oncol.* 2016;6:29.
24. Lei H, Zhu XH, Zhang XL, Ugurbil K, Chen W. In vivo 31P magnetic resonance spectroscopy of human brain at 7 T: an initial experience. *Magn Reson Med.* 2003;49(2):199-205.
25. Du F, Zhu XH, Qiao H, Zhang X, Chen W. Efficient in vivo 31P magnetization transfer approach for noninvasively determining multiple kinetic parameters and metabolic fluxes of ATP metabolism in the human brain. *Magn Reson Med.* 2007;57(1):103-114.
26. Gilboe DD, Kintner DB, Anderson ME, Fitzpatrick JH Jr. NMR-based identification of intra-and extracellular compartments of the brain pi peak. *J Neurochem.* 1998;71(6):2542-2548.
27. Hendriks AD, Fracasso A, Arteaga de Castro CS, et al. Maximizing sensitivity for fast GABA edited spectroscopy in the visual cortex at 7 T. *NMR in biomedicine.* 2018;31(4):e3890.

28. Klomp DW, van der Graaf M, Willemsen MA, van der Meulen YM, Kentgens AP, Heerschap A. Transmit/receive headcoil for optimal ^1H MR spectroscopy of the brain in paediatric patients at 3 T. *Magma*. 2004;17(1):1-4.
29. Scheenen TW, Heerschap A, Klomp DW. Towards ^1H -MRSI of the human brain at 7T with slice-selective adiabatic refocusing pulses. *Magma*. 2008;21(1-2):95-101.
30. Pohmann R, von Kienlin M. Accurate phosphorus metabolite images of the human heart by 3D acquisition-weighted CSI. *Magn Reson Med*. 2001;45(5):817-826.
31. Kay KN, Winawer J, Rokem A, Mezer A, Wandell BA. A two-stage cascade model of BOLD responses in human visual cortex. *PLoS Comput Biol*. 2013;9(5):e1003079.
32. van de Bank BL, Orzada S, Smits F, et al. Optimized ^{31}P MRS in the human brain at 7 T with a dedicated RF coil setup. *NMR Biomed*. 2015;28(11):1570-1578.
33. Lagemaat MW, van de Bank BL, Sati P, Li S, Maas MC, Scheenen TW. Repeatability of ^{31}P MRSI in the human brain at 7 T with and without the nuclear Overhauser effect. *NMR Biomed*. 2016;29(3):256-263.
34. Khlebnikov V, Siero JCW, Bhogal AA, Luijten PR, Klomp DWJ, Hoogduin H. Establishing upper limits on neuronal activity-evoked pH changes with APT-CEST MRI at 7 T. *Magn Reson Med*. 2018;80(1):126-136.
35. van de Bank BL, Maas MC, Bains LJ, Heerschap A, Scheenen TWJ. Is visual activation associated with changes in cerebral high-energy phosphate levels? *Brain Struct Funct*. 2018;223(6):2721-2731.
36. Ren J, Shang T, Sherry AD, Malloy CR. Unveiling a hidden ^{31}P signal coresonating with extracellular inorganic phosphate by outer-volume-suppression and localized ^{31}P MRS in the human brain at 7T. *Magn Reson Med*. 2018;80(4):1289-1297.
37. Boer VO, van de Lindt T, Luijten PR, Klomp DW. Lipid suppression for brain MRI and MRSI by means of a dedicated crusher coil. *Magn Reson Med*. 2015;73(6):2062-2068.
38. Mangia S, Tkac I, Gruetter R, Van de Moortele PF, Maraviglia B, Ugurbil K. Sustained neuronal activation raises oxidative metabolism to a new steady-state level: evidence from ^1H NMR spectroscopy in the human visual cortex. *J Cereb Blood Flow Metab*. 2007;27(5):1055-1063.

How to cite this article: Hendriks AD, van der Kemp WJM, Luijten PR, Petridou N, Klomp DWJ. SNR optimized ^{31}P functional MRS to detect mitochondrial and extracellular pH change during visual stimulation *NMR in Biomedicine* 2019;32:e4137. <https://doi.org/10.1002/nbm.4137>